

Quantum-to-Classical Transition of Proton-Transfer in Electrocatalytic Oxygen Reduction

Ken Sakaushi,*^[a,b] Andrey Lyalin,^[b] Tetsuya Taketsugu,^[b,c] and Kohei Uosaki^[a,b]

[a] Center for Green Research on Energy and Environmental Science, National Institute for Materials Science, Namiki 1-1, Tsukuba, Ibaraki, 305-0044 (Japan)

[b] Global Research Center for Environment and Energy based on Nanomaterials Science, National Institute for Materials Science, Namiki 1-1, Tsukuba, Ibaraki 305-0044 (Japan)

[c] Department of Chemistry, Faculty of Science, Hokkaido University, Sapporo 060-0810 (Japan)

AUTHOR INFORMATION

Corresponding Author: Sakaushi.ken@nims.go.jp

Abstract: The four-electron oxygen reduction reaction (ORR; $\text{O}_2 + 2\text{H}_2\text{O} + 4e^- \rightarrow 4\text{OH}^-$) on Pt catalyst in alkaline solution undergoes proton transfer *via* tunneling mechanism. The hydrogen/deuterium kinetic isotopic rate constant ratio ($k_{\text{H}}/k_{\text{D}}$) = 33 in a low overpotential (η) region, indicating the importance of the quantum-proton-tunneling at the rate-determining step (RDS). However, $k_{\text{H}}/k_{\text{D}}$ goes down to 4.1 in a high η region, suggesting the classical proton-transfer (PT) scheme. Therefore, there is a quantum-to-classical transition of PT process as a function of potential, which is confirmed by theoretical study. This observation indicates that PT is involved to the RDS of ORR on Pt in alkaline condition, and also shows that quantum tunneling rules the electrochemical reduction of oxygen in low η condition. The electrode process reported here can support to unveil highly complicated microscopic mechanism of energy-conversion reactions.

Multielectron-, and multiproton-transfer reactions play vital roles in a wide spectrum of energy storage/conversion reactions working in biological systems and also for modern device,^[1] such as fuel-cells and rechargeable batteries. Unveiling their complicated microscopic mechanisms can give huge impacts for basic science. For example, this can help to understand efficient reaction pathways in nature, and therefore, these knowledge can advance important energy-oriented technologies, for instance, designing highly-active catalysts based on non-traditional approaches.^[2]

Electrochemical oxygen activation is a key chemistry among the reactions related to proton- and electron-transfer because it is fundamental for other oxygen-related reactions, and also, its sluggish kinetics is the central issue of various energy technology.^[3] The possible mechanisms of the oxygen reduction reaction (ORR) have been intensively studied both theoretically and experimentally. There are several candidates for initial activation process of dioxygen molecule on Pt surfaces being described by several steps containing rate-determining step (RDS) under the Parsons' hypothetical framework of electrode kinetics based on transition state theory. These steps are indeed the key for the whole process, where four electrons and four protons are transferred into a dioxygen molecule in total. There are several possible candidates for the RDS of ORR. From experimental results,^[4] concerted-proton-electron transfer was suggested to be a possible candidate of RDS. In addition to this, theoretical and experimental works suggested that the formation/desorption of intermediates, such as $(O)_{ads}$, $(OOH)_{ads}$ or $(OH)_{ads}$, can control the RDS of noble-metal-based materials.^[5]

There are many basic concepts for theoretical and empirical ORR models,^[5a, 6] however, they are still not able to explain adequately the comprehensive experimental observations. Therefore,

finding out elementary steps and the RDS of electrochemical oxygen activation process is of great interest and importance. One of the simplest approaches to investigate this issue is to measure hydrogen/deuterium kinetic isotopic rate constant ratio $k_{\text{H}}/k_{\text{D}}$ ($K^{\text{H/D}}$).^[7] By measuring $K^{\text{H/D}}$, we can clarify the participation of proton-transfer (PT) processes in a RDS. Although there are many experimental and theoretical reports on kinetic isotope effect (KIE) in organic- and bio-chemical reactions,^[8] and several researchers suggested the importance of tunneling effect in electrochemical reactions,^[9] the KIE in the electrocatalytic ORR is not well known and poorly understood.^[10] This fact drove us to obtain $K^{\text{H/D}}$ values on the common Pt catalysts in a variety of conditions.

Herein, we show that $K^{\text{H/D}} = 33$ on Pt in alkaline condition and this value drops down to 4.1 as a function of potential, indicating quantum-to-classical transition. This suggests that a proton tunneling can play an important role for the RDS of ORR: at lower overpotential condition, proton prefers to be transferred by quantum-tunneling (Scheme 1). This result shows an undiscovered insights on a key reaction to develop both experiments and theory for unveiling its microscopic description on complicated multistep-, multielectron-transfer processes. For this study, polycrystalline Pt disk-electrode (pcPt) were used as a model catalyst. We put a special care to conduct electrochemical experiments since alkaline solution is easy to get contamination. For this reason, the use of ultrapure heavy water is important. Furthermore, in order to confirm that our electrochemical system can measure activities correctly, we checked the activity of a polycrystalline gold electrode with the Damjanovic model and succeeded to reproduce the previous report using alkaline electrolyte (Figure S1).^[11] Indeed, as shown later, the purity of electrolyte was checked by rotating-disk electrode technique.^[12]

Figure 1a shows the CV of pcPt in Ar-saturated pH13 (0.1M KOH in H₂O) and pD13 (0.1M KOD in D₂O) solutions, respectively. The potentials versus the reversible hydrogen electrode (RHE) in this manuscript are specified as V_{RHE} . The peaks corresponding to the under-potential deposition (UPD) of deuteron to Pt surface shift compared to the H-UPD peaks. For example, the H-UPD peaks located at 0.31 V_{RHE} and 0.41 V_{RHE} shift to 0.26 V_{RHE} and 0.37 V_{RHE} , respectively (Figure 1a). The H-UPD peaks on pcPt surfaces in pH13 are identical to the previous experiments.^[13] The D-UPD peaks have slightly broad feature compared to proton ones, which was also observed by previous report^[10a], and also, for the case of acidic condition (Figure S4). Indeed, the peak positions of OH⁻ adsorption, oxide formation/reduction are shifted as well. This effect can be explained by the difference in adsorption energy of the deuterated compounds, such as deuteron and OD⁻, compared to the protonated ones. Furthermore, even in a wider potential window, deuterium evolution/oxidation reactions cannot be observed in pD13 but hydrogen evolution/oxidation reaction can be clearly observed in pH13. As it was reported by previous theoretical analysis on electrochemical proton-transfer mechanism based on models, such as the Dogonazde-Kuznetsov-Levich approach,^[14] or ones combined with the Marcus-Hush theory,^[15] the reactions related to deuteron-transfer can demonstrate different kinetics compared to the proton-transfer-related reactions. Therefore, this difference should be corrected in order to discuss KIE of ORR and this is the reason why the new equations and the basic kinetic parameters, such as exchange current density (J_0), should be obtained.

In order to check the details of the reaction kinetics, linear-sweep voltammetry (LSV) combined with rotating disk electrode (RDE) technique was applied (Figure 1b). We checked the shapes of deuteron desorption peaks in Ar-saturated condition with and without rotation and confirmed that those shapes are same (Figure S2). This result guarantees that the validity of above

experiment.^[12] In order to discuss kinetic values, three courses of same experiments are operated and we show average values of Tafel slopes with standard errors in the figures. As shown in these figures, standard errors are small enough to discuss the electrode mechanism. We used geometrical surface-area to calculate current density. Since the physical quantities, such as oxygen diffusion and kinetic viscosity, are different in H₂O and D₂O, the diffusion limiting current density (J_{diff}) changes in pH13 and pD13. Therefore, we calculate J_{diff} in pH13 ($J_{\text{diff}}^{\text{H}}$) and in pD13 ($J_{\text{diff}}^{\text{D}}$) by using the Levich equation (see SI) to obtain theoretical ratio of $J_{\text{diff}}^{\text{H}}$ and $J_{\text{diff}}^{\text{D}}$, and this was calculated as $J_{\text{diff}}^{\text{D}}/J_{\text{diff}}^{\text{H}} = 0.93$, which is very close to the experimentally obtained $J_{\text{diff}}^{\text{D}}/J_{\text{diff}}^{\text{H}}$ being 0.89 ± 0.02 (Figure 1b). Indeed, average electron transfer numbers to O₂ of in both conditions are about 4.0, which is a typical value for the Pt surfaces in alkaline conditions, suggesting the proper ORR measurements in both D₂O and H₂O (Figure S3).

Since $K^{\text{H/D}}$ is defined as the ratio of the isotopic rate constants, one can obtain this value from following equations:

$$K^{\text{H/D}} = \frac{J_0^{\text{H}}}{J_0^{\text{D}}} \times \frac{C_0^{\text{D}}}{C_0^{\text{H}}} \quad (\text{Eq. 1})$$

$$J = J_0 \exp\left(\frac{\alpha F}{RT} \eta\right) \quad (\text{Eq. 2})$$

where C_0 , α , η , F , R and T are, oxygen concentration, transfer coefficient, overpotential, Faraday constant, gas constant and temperature (298 ± 1 K in this experiment), respectively. The potential difference due to different thermodynamic properties for ORR in heavy and ordinary water ($\Delta\phi$) and the equilibrium potential for D₂O formation ($E^0_{\text{D}_2\text{O}}$) can be calculated by thermophysical values, which can be found in the ref. 6 in the ref 10a of this report, and we obtain $\Delta\phi = -0.02$ V and $E^0_{\text{D}_2\text{O}} = 1.249$ V_{RHE} since the equilibrium potential of deuterium evolution reaction is -0.013 V_{RHE}. Transfer coefficient α can be obtain from the Tafel slope (b):

$$\frac{2.3RT}{\alpha F} = b. \quad (\text{Eq. 3})$$

The ORR kinetics in pH13 and pD13 were analyzed by focusing on the kinetic-control region (Figure 2 and Table 1). The kinetic-control region was found by comparing the LSV curves with different rotation speeds in order to check the potential region without effects of O₂ diffusion (Figure S7-S12). The value of the Tafel slope b was confirmed to be around 0.05 V/dec in a low η region (Region I) and shifted to 0.07 V/dec at a middle η region (Region II). The Regions are decided by following the previous report.^[16] Although exact reason for this change of b is still an open question, this is well-known phenomena,^[17] and the Tafel slope values are same as previous observation.^[13]

From the Eq.1, 2, 3 and Table 1, $K^{H/D}$ of pcPt in Region I and II can be obtained as 33 and 9, respectively. From this result, it indicates that the RDS of ORR in alkaline condition contains proton transfer. Indeed, anomalous value of $K^{H/D} > 13$ indicates quantum-proton-tunneling, which is a classically forbidden proton-transfer mechanism. This is because the maximum KIE for the O-H bond is 13 in 298 K based on the semi-classical theory (see the ref. 7b, p.83). On the other hand, from the data obtained in the acidic condition (Figure S4, S5), $K^{H/D}$ is 1, comparing values from 0.05M D₂SO₄ (pD1) and 0.05M H₂SO₄ (pH1) solutions (Figure S6 and Table S1). This indicates that proton-transfer is not related in the RDS of ORR in acidic condition. This fact shows that the ORR in acidic condition follows the traditional scheme suggesting that the first electron transfer to adsorbed O₂ may be the RDS since a previous careful and detailed study on KIE of ORR using phosphoric acid also reported that $K^{H/D} = 1$.^[10a] We note here that pcPt seems to exhibit better kinetics in 0.05M D₂SO₄ solution compared to 0.05M H₂SO₄ solution with simple LSV experiment in V_{RHE} scale (Figure S5), however this is because it is not converted to the

overpotential scale. If J_0 is obtained from the overpotential vs. $\log J_k$ diagram (Figure S6) and this value is applied to Eqs. 1, 2 and 3, one can find that there is no isotopic effect. In other words, correct KIE cannot be obtained without adjustment of different thermodynamic potential in the heavy water system compared to the ordinary one.

The Koutecky-Levich (K-L) equation (see SI) was applied to analyze the KIE in kinetics-diffusion-mixed region (Region III in Figure 2) being much higher overpotential region compared to Region I and II. A series of LSV measurements with a variety of rotating speeds was carried out in order to apply the K-L equation (Figure S7-S12), and obtain a variety of J_k with a function of potential by K-L plots (Figure S13-18). In case of pD13, the Region III is from 0.90 to 0.80 V_{RHE} , and from 0.95 to 0.85 V_{RHE} in case of pH13. From the K-L plots, the average electron transfer numbers to O_2 can be determined as 3.96 and 3.92 in pH13 and pD13, respectively. This result well agrees with the value obtained by rotating-ring disk technique (Figure S3). The Tafel plots in the Region III can be obtained by using J_k calculated from K-L plots and all kinetic data is summarized in Table 1. The Tafel slopes of pcPt for both conditions were again confirmed to be 0.2 V/dec, which is the same value as was reported in previous works.^[13] By using Eqs. 1 and 2, the $K^{H/D}$ of pcPt in the Region III was found to be 4.1, which is much lower than the value obtained at Region I ($K^{H/D} = 33$) and comparable to II ($K^{H/D} = 9$). By combining previous reports,^[3b, 3c, 4, 5c, 5e, 6b, 6c, 7b] and our experimental observations, it can be concluded that proton-transfer process is related to the rate-determining step of ORR in alkaline conditions. Although there are several candidates for the RDS in alkaline solution, which are based on PT from adsorbed water molecule or from solution (see SI Note S3), PT to $(O)_{ads}$ is selected as RDS since it is possible rate-determining steps suggested by experiment/computational calculations and are consisted of bond-braking/-formation with proton, which is O-H bond braking of H_2O and then

formation of O-H bond. Based on the above considerations, we analyzed our experimental results by using a theoretical approach.

A simple expression for the rate constant $k(T)$ can be written as

$$k(T) = A/k_B T \int_0^\infty P(E) e^{-E/k_B T} dE \quad (\text{Eq. 4})$$

where A is a rate constant frequency factor, k_B is Boltzmann's constant, and $P(E)$ is the barrier permeability at energy E .^[8a, 8b] In the present work we approximate the barrier for proton transfer by the asymmetric Eckart's one-dimensional potential energy function,^[7b]

$$V(r) = \left[(V_1)^{\frac{1}{2}} + (V_1 + \Delta V)^{\frac{1}{2}} \right]^2 / 4 \cosh^2 \left(\frac{r}{a} \right) - \Delta V e^{\frac{r}{a}} / 2 \cosh \left(\frac{r}{a} \right), \quad (\text{Eq. 5})$$

where V_1 is the barrier height, ΔV is reaction exothermicity, and a is the barrier width parameter. In the case of the Eckart potential (Eq. 5), the barrier permeability $P(E)$ can be evaluated analytically or numerically by solving corresponding Schrödinger's equation (see Note S4). In the case of the electrochemical reaction, parameters of the reaction barrier height and exothermicity can be altered via applied potentials. In the present work the Brønsted-Evans-Polanyi relationship was used to describe linear variations in the barrier height with the reaction energy,

$$V_1 = -A\Delta V + B, \quad (\text{Eq. 6})$$

where A characterizes the position of the transition state along the reaction coordinate, herein taken to be 0.5, and B is the barrier height at the equilibrium, *i.e.* when $\Delta V=0$.^[5e] Substituting (Eq. 6) in (Eq. 5) we have calculated the $K^{\text{H/D}}$ for the proton transfer from the water molecule to $(\text{O})_{\text{ads}}$ as one of the most probable RDS processes with the use of computer code described by Le Roy.^[8b] It should be noted that the tunneling probability is strongly affected by the barrier width (Figure S19). We estimated the barrier width parameter a to be equal 0.3 Å using theoretical data on the optimized structures for the adsorption of the reaction intermediates covered by bilayer of water on Pt(111) surface^[5h] (see Note S5). The value of the barrier height B for the proton-transfer for the steps at the equilibrium is open-to-debate, and the reported values vary from 0.26 to 0.81 eV.^[5d, 5e, 5g] Therefore, we have calculated the dependence of $\log K^{\text{H/D}}$ on exothermicity (ΔV) for the several available values of the proton transfer barrier at equilibrium as it is shown in Figure 3a. Results of our theoretical analysis demonstrate that for the small values of ΔV tunneling effect dominates in the proton transfer in a good agreement with the experimental observation (Figure 3b). It is interesting that for $B = 0.74$ eV reported by Sugino et al,^[5g] the $K^{\text{H/D}}$ is equal to 1.76 which is very close to the experimentally observed value of 1.51. Both theoretical and experimental results demonstrate that tunneling can be observed in the low overpotential regime while proton transfer process becomes classical one at high overpotentials. Our combined-theoretical/experimental study clearly demonstrates manifestation of the potential-dependent KIE in electrochemical system processes. The observed quantum-to-classical transition in the proton-transfer mechanism as a function of the potential shows that the tunneling mechanism dominates in the proton transfer in the low η region because it is more energetically beneficial than overcoming the activation barrier. However, in high η region, the barrier becomes low enough and therefore the classical proton-transfer mechanism controls the overall process.

In conclusion, we have shown that there is a quantum-to-classical transition in electrochemical oxygen reduction in alkaline solution. On the other hand, $K^{H/D}$ is 1 from low to high overpotential region in the case of acidic condition, suggesting PT is not related to RDS. Likewise unexpected strong effects of adsorbed ions or crystal structures for electrode processes,^[6b, 12] this study indicates that the non-trivial importance of proton-transfer in electrochemical oxygen reduction. Especially, proton-transfer mechanism is indeed different in acid and alkaline conditions, we believe that understanding of quantum proton-transfer mechanism is key to clarify the fundamental principles in complicated electrode processes. Since the detailed microscopic mechanism of ORR is still unclear, the quantum effect and the analytical approach based on KIE shown here can be an additional tool to obtain new insights of this process in order to build more accurate theoretical models and combine them to experimental systems to unveil the complicated electrode process.

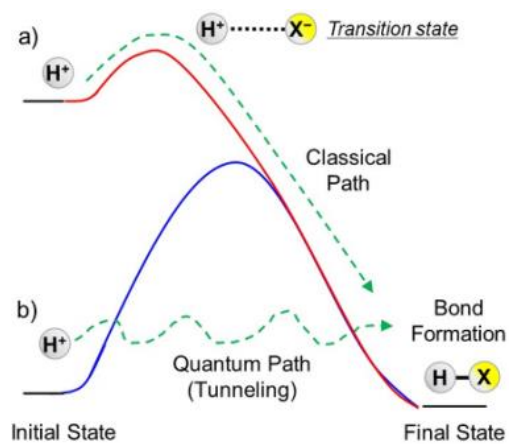
Acknowledgements

K.S. is indebted to NIMS, and to Program for Development of Environmental Technology using Nanotechnology by MEXT for supports. This work was financially supported by JSPS KAKENHI Grants 15H06850, 15K05387, 16KT0047 and 17K14546, and partly supported by MEXT as "Priority Issue on Post-K computer" (Development of new fundamental technologies for high-efficiency energy creation, conversion/storage and use). K.S. thanks to Mr. Markus Eckardt and Prof. Dr. R. Jürgen Behm (Ulm University) for supporting experiment, and the anonymous researcher for fruitful comments. Prof. Robert J. Le Roy is deeply acknowledged for providing us his original code described in the ref. 8b.

[1] a) V. R. Stamenkovic, D. Strmcnik, P. P. Lopes, N. M. Markovic, *Nat. Mater.* **2017**, *16*, 57-69; b) A. Kohen, J. P. Klinman, *Acc. Chem. Res.* **1998**, *31*, 397-404.

- [2] a) G. Ertl, *Angew. Chem. Int. Ed.* **2008**, 47, 3524-3535; b) J. Sauer, H.-J. Freund, *Catal. Lett.* **2014**, 145, 109-125; c) K. Sakaushi, M. Antonietti, *Acc. Chem. Res.* **2015**, 48, 1591-1600; d) K. Sakaushi, A. Lyalin, S. Tominaka, T. Taketsugu, K. Uosaki, *ACS Nano* **2017**, 11, 1770-1779.
- [3] a) A. Frumkin, V. Bagotskii, Z. Iofa, B. Kabanov, *Kinetics of Electrode Processes*, Moscow State Univ., Moscow, 1952; b) M. Tarasevich, A. Sadkowski, E. Yeager, *Oxygen Electrochemistry In Comprehensive Treatise of Electrochemistry* (Eds.: B. E. Conway, J. O. M. Bockris, E. Yeager, S. U. M. Khan, R. E. White), Springer US, Boston 1983, 301-398; c) R. Adzic, Recent advances in the kinetics of oxygen reduction In *Electrocatalysis* (Eds.: J. Lipkowski, P. N. Ross), Wiley-VCH: New York, 1998.
- [4] M. T. M. Koper, *Chem. Sci.* **2013**, 4, 2710-2723.
- [5] a) J. K. Nørskov, J. Rossmeisl, A. Logadottir, L. Lindqvist, J. R. Kitchin, T. Bligaard, H. Jónsson, *J. Phys. Chem. B* **2004**, 108, 17886-17892; b) F. Abild-Pedersen, J. Greeley, F. Studt, J. Rossmeisl, T. R. Munter, P. G. Moses, E. Skúlason, T. Bligaard, J. K. Nørskov, *Phys. Rev. Lett.* **2007**, 99, 016105; c) J. Rossmeisl, G. S. Karlberg, T. Jaramillo, J. K. Nørskov, *Faraday Discuss.* **2009**, 140, 337-346; d) M. J. Janik, C. D. Taylor, M. Neurock, *J. Electrochem. Soc.* **2009**, 156, B126-B135; e) V. Tripković, E. Skúlason, S. Siahrostami, J. K. Nørskov, J. Rossmeisl, *Electrochim. Acta* **2010**, 55, 7975-7981; f) I. E. L. Stephens, A. S. Bondarenko, F. J. Perez-Alonso, F. Calle-Vallejo, L. Bech, T. P. Johansson, A. K. Jepsen, R. Frydendal, B. P. Knudsen, J. Rossmeisl, I. Chorkendorff, *J. Am. Chem. Soc.* **2011**, 133, 5485-5491; g) N. Bonnet, M. Otani, O. Sugino, *J. Phys. Chem. C* **2014**, 118, 13638-13643; h) S. Liu, M. G. White, P. Liu, *J. Phys. Chem. C* **2016**, 120, 15288-15298; i) M. F. Li, L. W. Liao, D. F. Yuan, D. Mei, Y.-X. Chen, *Electrochim. Acta* **2013**, 110, 780-789.
- [6] a) R. R. Dogonadze, A. M. Kuznetsov, *Quantum Electrochemical Kinetics: Continuum Theory in Comprehensive Treatise of Electrochemistry: Volume 7 Kinetics and Mechanisms of Electrode Processes* (Eds.: B. E. Conway, J. O. M. Bockris, E. Yeager, S. U. M. Khan, R. E. White), Springer US, Boston 1983, pp. 1-40; b) N. M. Marković, P. N. Ross, *Surf. Sci. Rep.* **2002**, 45, 117-229; c) A. B. Anderson, *Phys. Chem. Chem. Phys.* **2012**, 14, 1330-1338; d) R. Jinnouchi, K. Kodama, T. Hatanaka, Y. Morimoto, *Phys. Chem. Chem. Phys.* **2011**, 13, 21070-21083; e) A. Ignaczak, R. Nazmutdinov, A. Goduljan, L. Moreira de Campos Pinto, F. Juarez, P. Quaino, E. Santos, W. Schmickler, *Nano Energy* **2016**, 26, 558-564.
- [7] a) R. P. Bell, *Proc. Royal Soc. A* **1936**, 154, 414-429; b) R. P. Bell, *The tunnel effect in chemistry*, Springer, 1980.
- [8] a) P. H. Cribb, S. Nordholm, N. S. Hush, *Chem. Phys.* **1978**, 29, 43-54; b) R. J. Le Roy, H. Murai, F. Williams, *J. Am. Chem. Soc.* **1980**, 102, 2325-2334; c) Y. Cha, C. Murray, J. Klinman, *Science* **1989**, 243, 1325-1330; d) A. M. Kuznetsov, J. Ulstrup, *Can. J. Chem.* **1999**, 77, 1085-1096; e) M. J. Knapp, K. Rickert, J. P. Klinman, *J. Am. Chem. Soc.* **2002**, 124, 3865-3874; f) E.

- Hatcher, A. V. Soudackov, S. Hammes-Schiffer, *J. Am. Chem. Soc.* **2004**, 126, 5763-5775; g) J. Bonin, C. Costentin, M. Robert, J.-M. Savéant, C. Tard, *Acc. Chem. Res.* **2012**, 45, 372-381; h) S. Hammes-Schiffer, *J. Am. Chem. Soc.* **2015**, 137, 8860-8871.
- [9] a) C. E. H. Bawn, G. Ogden, *Trans. Faraday Soc.* **1934**, 30, 432-443; b) S. G. Christov, *Z. Elektrochem.* **1958**, 62, 567-581; c) J. O. M. Bockris, D. B. Matthews, *J. Chem. Phys.* **1966**, 44, 298-309.
- [10] a) M. M. Ghoneim, S. Clouser, E. Yeager, *J. Electrochem. Soc.* **1985**, 132, 1160-1162; b) D. Mei, Z. D. He, Y. L. Zheng, D. C. Jiang, Y.-X. Chen, *Phys. Chem. Chem. Phys.* **2014**, 16, 13762-13773; c) E. C. M. Tse, J. A. Varnell, T. T. H. Hoang, A. A. Gewirth, *J. Phys. Chem. Lett.* **2016**, 7, 3542-3547.
- [11] R. W. Zurilla, R. K. Sen, E. Yeager, *J. Electrochem. Soc.* **1978**, 125, 1103-1109.
- [12] N. M. Marković, R. R. Adžić, B. D. Cahan, E. B. Yeager, *J. Electroanal. Chem.* **1994**, 377, 249-259.
- [13] N. M. Marković, H. A. Gasteiger, P. N. Ross, *J. Phys. Chem.* **1996**, 100, 6715-6721.
- [14] R. R. Dogonadze, A. M. Kuznetsov, V. G. Levich, *Electrochim. Acta* **1968**, 13, 1025-1044.
- [15] a) N. S. Hush, *Trans. Faraday Soc.* **1961**, 57, 557-580; b) R. A. Marcus, *Annu. Rev. Phys. Chem.* **1964**, 15, 155-196.
- [16] J. X. Wang, N. M. Markovic, R. R. Adzic, *J. Phys. Chem. B* **2004**, 108, 4127-4133.
- [17] a) T. V. Albu, A. B. Anderson, *Electrochim. Acta* **2001**, 46, 3001-3013; b) N. M. Marković, H. A. Gasteiger, B. N. Grgur, P. N. Ross, *J. Electroanal. Chem.* **1999**, 467, 157-163.



Scheme 1. Schematic diagram for two possible paths of the proton-transfer reaction: a) proton transfer *via* transition state (classical); b) proton tunneling through the barrier (quantum). In the electrochemical system relative contribution of the two mechanisms can be tuned by the applied potential.

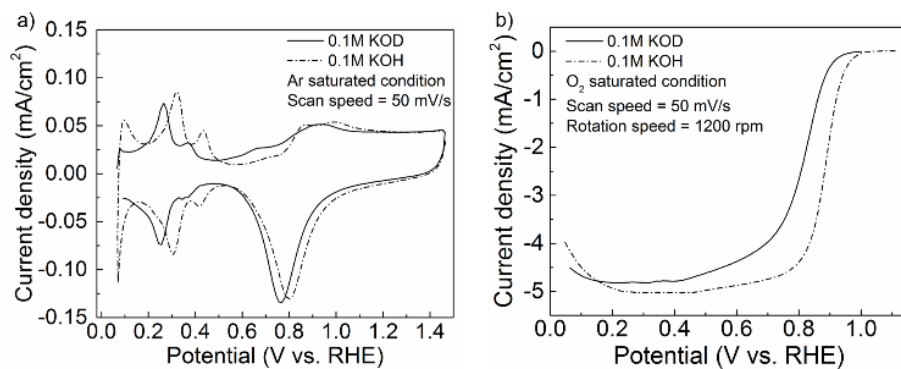


Figure 1. a) CV of pcPt in Ar-saturated condition and b) LSV curve with rotation at 1200 rpm in O₂-saturated condition. Solid and dotted lines indicate measurements in 0.1M KOD and 0.1M KOH, respectively. Scan speed is 50 mV/s. LSV was scanned from negative to positive potential.

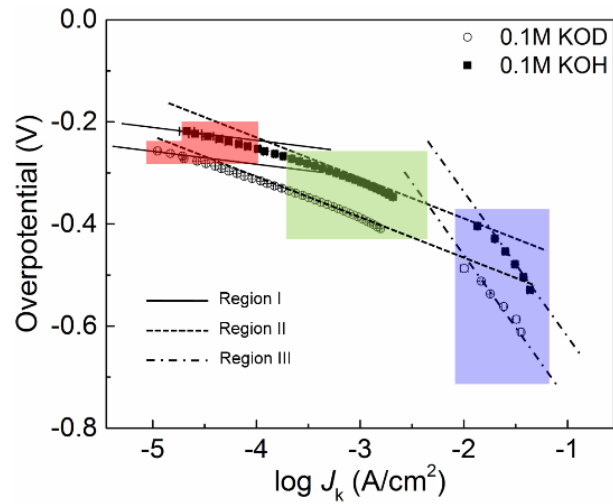


Figure 2. Overpotential vs. $\log J_k$ diagram of pcPt in O₂-saturated 0.1 M KOD and 0.1M KOH solutions. Three different regions are selected to take Tafel slope: Region I (Red area, lower overpotential), Region II (Green area, middle overpotential) and Region III (Blue area, higher overpotential). Plots in Regions I and II are obtained from LSV (50 mV/s) with 900 rpm. Plots in Region III were obtained by K-L plots.

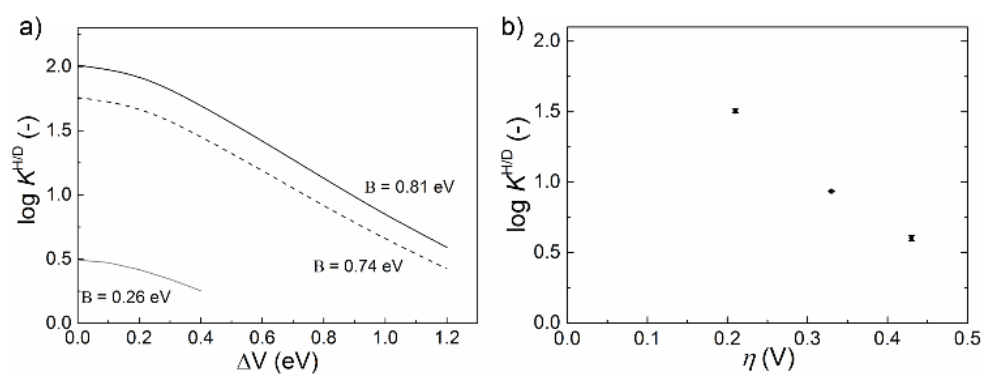


Figure 3. a) Dependence of $\log K^{H/D}$ on the reaction exothermicity (ΔV), calculated for the values of the proton transfer barrier at equilibrium $B = 0.26$ eV,^[5e] 0.74 eV,^[5g] and 0.81 eV^[5d] reported in literature. b) Experimentally obtained $\log K^{H/D}$ vs. η plots.

Table 1. Summary of ORR kinetics and $K^{H/D}$

| Region | Tafel slope (V/dec) | α | $-\log J_0^H$ (A/cm ²) | $-\log J_0^D$ (A/cm ²) | $K^{H/D}$ |
|--------|---------------------|----------|------------------------------------|------------------------------------|------------|
| I | 0.046 ± 0.005 | 1.3 | 9.48 ± 0.55 | 10.95 ± 0.22 | 32.5 ± 1.5 |
| II | 0.068 ± 0.003 | 0.88 | 7.66 ± 0.09 | 8.57 ± 0.03 | 8.6 ± 0.2 |
| III | 0.22 ± 0.02 | 0.27 | 3.64 ± 0.13 | 4.1 ± 0.21 | 4.1 ± 0.3 |